Vapor-liquid interfacial properties of fully flexible Lennard-Jones chains

Felipe J. Blas,[1,a)] Luis G. MacDowell,[2] Enrique de Miguel,[1] and George Jackson[3]
[1]*Departamento de Física Aplicada, Facultad de Ciencias Experimentales, Universidad de Huelva, 21071 Huelva, Spain*
[2]*Departamento de Química-Física, Facultad de Ciencias Químicas, Universidad Complutense de Madrid, 28040 Madrid, Spain*
[3]*Department of Chemical Engineering, Imperial College London, South Kensington Campus, London SW7 2AZ, United Kingdom*

(Received 16 July 2008; accepted 5 September 2008; published online 14 October 2008)

We consider the computation of the interfacial properties of molecular chains from direct simulation of the vapor-liquid interface. The molecules are modeled as fully flexible chains formed from tangentially bonded monomers with truncated Lennard-Jones interactions. Four different model systems comprising of 4, 8, 12, and 16 monomers per molecule are considered. The simulations are performed in the canonical ensemble, and the vapor-liquid interfacial tension is evaluated using the test area and the wandering interface methods. In addition to the surface tension, we also obtain density profiles, coexistence densities, critical temperature and density, and interfacial thickness as functions of temperature, paying particular attention to the effect of the chain length on these properties. According to our results, the main effect of increasing the chain length (at fixed temperature) is to sharpen the vapor-liquid interface and to increase the width of the biphasic coexistence region. As a result, the interfacial thickness decreases and the surface tension increases as the molecular chains get longer. The interfacial thickness and surface tension appear to exhibit an asymptotic limiting behavior for long chains. A similar behavior is also observed for the coexistence densities and critical properties. Our simulation results indicate that the asymptotic regime is reached for Lennard-Jones chains formed from eight monomer segments. We also include a preliminary study on the effect of the cutoff distance on the interfacial properties. Our results indicate that all of the properties exhibit a dependence with the distance at which the interactions are truncated, though the relative effect varies from one property to the other. The interfacial thickness and, more particularly, the interfacial tension are found to be strongly dependent on the particular choice of cutoff, whereas the density profiles and coexistence densities are, in general, less sensitive to the truncation. © *2008 American Institute of Physics*. [DOI: 10.1063/1.2989115]

I. INTRODUCTION

Interfacial phenomena play a key role not only in many scientific fields such as nucleation, nanotechnology, or the dynamics of phase transitions, but also in a great number of practical applications. Solubilization of immiscible fluids, detergency, lubricants, and the design of lyotropic liquid-crystalline amphiphiles for use as soaps, cosmetics, and foodstuffs are some common applications where an understanding of the interfacial properties is essential.

From a microscopic point of view, interfacial problems can be studied using well-established statistical mechanical tools, either molecular theories appropriate for inhomogeneous systems[1–3] or molecular simulation techniques,[4,5] which are also routinely used to examine inhomogeneous systems. In this work we focus on this second approach and use Monte Carlo (MC) simulation to determine the interfacial properties of the planar vapor-liquid interface of molecular chain models.

Thermodynamic and structural properties play an essential role in the description of the interface in inhomogeneous systems, including density profiles, bulk coexistence densities, the interfacial thickness, surface tension, and orientational and positional order along the interface. Although all of these properties are relevant for the characterization of the interfacial behavior, the surface tension is arguably the most important and interesting interfacial property.

There are basically three different routes to the calculation of the surface tension from simulation. We describe these briefly here and refer the reader to recent comprehensive reviews.[6–8] The first class of techniques involves the calculation of the pressure tensor of the inhomogeneous system. For systems with planar vapor-liquid interfaces, the surface tension can be readily expressed in terms of the difference between the normal and tangential tensorial components of the pressure, these components being defined with respect to a frame where one of the axes is perpendicular to the interface. The most widespread method for the calculation of the components of the pressure tensor invokes the virial relation of Kirkwood and co-workers.[9,10] This requires an explicit calculation of the intermolecular forces so that the virial route is particularly appealing when molecular dynamics is the simulation technique of choice. Alternatively, the components of the pressure tensor can also be obtained directly from the formal thermodynamic expression

a)Electronic mail: felipe@uhu.es.

that relates the pressure (in this case the components of the pressure tensor) to the first-order derivative of the Helmholtz free energy with respect to the volume.[11–14] The corresponding derivatives can be accurately computed from an evaluation of the change in free energy associated with appropriate small volume perturbations.

The second route to the calculation of the surface tension is based on the concepts of finite-size scaling.[15] One of the most widely used techniques is due to Binder.[15] It relies on an estimation of the Landau free-energy barrier between the two coexisting phases, which is ultimately related to the interfacial tension. One typically considers a series of different system sizes, and a finite-size scaling analysis is then used to extract the value of the interfacial tension in the limit of an infinite system size. This methodology is adequate at high temperatures close to the critical region, where the large density fluctuations allow one to sample the two (liquid and vapor) coexisting phases. However, as the temperature is lowered from the critical temperature, sampling density fluctuations become increasingly difficult and the method is less efficient. A number of variations of the method have been devised in order to enhance the efficiency of the sampling in the low-temperature regime; further details can be found in Refs. 6, 7, and 16.

Finally, the third route to the calculation of the surface tension is based on its thermodynamic definition. The main strategy here is the computation of the free energy difference between two (or more) systems with different interfacial areas. This approach can be traced back to the work of Bennett,[17] Miyazaki *et al.*,[18] and Salomons and Mareschal.[19] Variants of this type of technique have been recently introduced. One is the so-called test-area (TA) technique proposed by Gloor *et al.*[7] This method allows one to calculate the surface tension from an evaluation of the change in free energy associated with a small, virtual change in the interfacial area at constant number of particles, volume, and temperature. MacDowell and Bryk[20] developed an alternative methodology based on the probability distribution of a wandering interface in which the interfacial area is allowed to randomly probe the available configurational space. The surface tension follows from the analysis of the corresponding interfacial area histogram. The last methodology is based on the expanded ensemble proposed by Lyubartsev *et al.*,[21] which is designed to efficiently calculate the free energy difference between two systems. Very recently, this technique was used independently by de Miguel[22] and Errington and Kofke[8] for the calculation of the free-energy difference between two inhomogeneous systems with the same number of particles, volume, and temperature, but a different interfacial area. This technique has been used to calculate the interfacial tension of the planar vapor-liquid interface of a number of molecular models (see the recent work of de Miguel[22] for further details).

Applications of these methods based on the thermodynamic definition of the surface tension have been reported for a wide range of intermolecular model potentials, including the Lennard-Jones (LJ),[7,20] square–well,[7,20,22] Gay–Berne,[7,22] several models of water,[23] the Widom–Rowlinson model,[24] as well as hard-sphere and bead-spring LJ chains.[20] The TA method, in combination with the standard mechanical (virial) route, has recently been used to calculate the surface tension of several alkanes[25] and acid gases.[26]

Whereas the computation of interfacial properties of polymer models has been the subject of a number of recent papers,[6,27–30] results for the well–known fully flexible LJ model, in which LJ segments (monomers) are tangentially bonded to form molecular chains, are scarce. The bulk thermodynamic properties of this model have been studied extensively by simulation, including not only the vapor-liquid phase behavior[31–34] but also the solid-fluid equilibria.[35–37] A knowledge of the interfacial properties of this model is much more limited, however. To the best of our knowledge, the only study of this kind is the work carried out by Duque *et al.*,[38] who determined the surface tension of LJ dimers and fully flexible LJ chains formed from four monomers using molecular dynamics simulation.

The goal of the present work is to study the vapor-liquid interfacial properties of fully flexible LJ chains formed from 4, 8, 12, and 16 monomers using *NVT* MC simulation of inhomogeneous systems. From the corresponding density profiles, we determine properties such as the interfacial thickness and bulk coexistence densities; the latter allows us to determine the critical properties (temperature and density) of the models. We also estimate the dependence of the interfacial properties with the chain length and temperature, placing a special emphasis on the surface tension. We examine a spherically truncated (ST) potential model with a cutoff distance of $r_c=4\sigma$ and without long-range corrections (LRCs) in most of the simulations performed, and carry out an analysis of the effect of the cutoff distance of the interactions on the interfacial properties. We study the effect of varying the ST LJ cutoff distance on different interfacial properties, including the equilibrium density profiles, coexistence densities, interfacial thickness, and surface tension.

The rest of the paper is organized as follows. In the next section we briefly consider the molecular model and the simulation details used in this work. The results obtained in this work are described in Sec. III. Finally, in Sec. IV we present the main conclusions.

II. MODEL AND SIMULATION DETAILS

We consider chain molecules formed from m identical LJ sites (monomer segments) characterized by a diameter σ and dispersive energy ϵ. The molecules are considered to be fully flexible (i.e., no restrictions in either the bond or the torsional angles) with a fixed monomer-monomer bond distance of $L=\sigma$ (meaning that chains of tangent monomers are considered). In this model, each monomer of a chain interacts with all other monomers in the system (i.e., in the same molecule or in the other molecules) with the LJ potential $u^{\mathrm{LJ}}(r_{ij})$

$$u^{\mathrm{LJ}}(r_{ij}) = 4\epsilon\left[\left(\frac{\sigma}{r_{ij}}\right)^{12} - \left(\frac{\sigma}{r_{ij}}\right)^{6}\right], \tag{1}$$

where r_{ij} is the distance between site (monomer) i and site j. Sites i and j can be in different or in the same molecule, so

we are explicitly considering both intermolecular and intramolecular interactions. The interactions are ST but not shifted at a given distance r_c. The explicit expression for the monomer-monomer interactions is

$$u_{\mathrm{ST}}^{\mathrm{LJ}}(r_{ij}) = u^{\mathrm{LJ}}(r_{ij})\Theta(r_c - r_{ij}) = \begin{cases} u^{\mathrm{LJ}}(r_{ij}) & r_{ij} \leq r_c, \\ 0 & r_{ij} > r_c, \end{cases} \quad (2)$$

where $\Theta(x)$ is the Heaviside step function. No LRCs are applied and most of the calculations are carried out considering a cutoff distance of $r_c=4\sigma$. In order to assess the effect of truncation on different interfacial properties, we also consider other values of cutoff distances, $r_c=3$ and 5σ, for selected thermodynamic conditions.

The number of molecules, N, used in each simulation depends on the chain length. We consider $N=504$, 252, 168, and 126 for systems formed from 4, 8, 12, and 16 monomers, respectively. This choice is made so as to have systems with the same total number of monomers irrespective of the particular chain length.

Code for the simulation of LJ dumbbells[39] is extended for the simulation of either rigid or flexible chain molecules in the *NVT*, *NPT*, or grand canonical ensemble in either bulk or a slit-pore geometry. Translational and rotational movements are supplemented with configurational bias displacements[40–42] and deletion/insertion attempts.[43] The energy is evaluated efficiently with the help of a link cell list. Further details of the specific implementation of configurational bias displacements and the cell list may be found elsewhere.[44,45]

Simulations are performed in the *NVT* ensemble. We consider a system of N molecules at a temperature T in a volume $V=L_xL_yL_z$, where L_x, L_y, and L_z are the dimensions of the rectangular simulation box. A homogeneous liquid system is first equilibrated in a rectangular simulation box of dimensions $L_x=L_y=11\sigma$ and $L_z=24$, 26, 28, and 30σ for systems with LJ chains formed from 4, 8, 12, and 16 monomers, respectively. In the case of fully flexible chains the end-to-end dimension of the chains is of the order of $\sim m^{1/2}$, which for the longest chains of $m=16$ studied corresponds to 4σ. The box is then expanded to three times its original size along the z direction while leaving the liquid phase at the center. On performing this expansion, care must be taken not to break chains spanning the periodic boundary conditions of the initial configuration. As a result, we obtain a centered liquid slab with the parts of the chains spanning across the boundary conditions of the original liquid configuration protruding into empty boxes of equal size at each side. The final overall dimensions of the vapor-liquid-vapor simulation box are therefore $L_x=L_y=11\sigma$ and $L_z=72$, 78, 84, and 90σ for the corresponding chain lengths.

All simulations are organized in cycles, where each cycle corresponds to N trial MC moves. Our MC procedure comprises three types of configurational updates: one involving a trial displacement of the molecular center of mass, and the other two, a partial and complete molecular regrowth of the molecular chains. For the latter, we consider a configurational bias scheme. Each type of move is chosen with a probability of 20%, 40%, and 40%, respectively. The magnitudes of the appropriate displacements are adjusted so as to get an acceptance rate of ~30% to 50%. We use periodic boundary conditions in all three directions of the simulation box.

The computation of the surface tension is accomplished either with the use of the TA or the wandering interface method (WIM). In particular, the surface tension of chains formed from 4 and 16 LJ monomers is calculated using the TA method, and that corresponding to the rest of systems is calculated using the WIM technique. In order to assess the consistency of both methods, we have calculated the surface tension of all the molecular systems with $r_c=3\sigma$ at two different temperatures using TA and WIM approaches. Results obtained with both methods are consistent (see Table VI for details) in all cases. The implementation of the TA technique involves performing area deformations of magnitude ΔA during the course of the simulation at constants N, V, and T every MC cycle. As shown by Gloor *et al.*,[7] the surface tension follows from the computation of the change in Helmholtz free energy associated with the perturbation, which in turn can be expressed as an ensemble average of the corresponding Boltzmann factor. Further details can be found in Ref. 7. We consider in all cases two perturbations of size $\Delta A^* = \Delta A / A_0 = \pm 0.0005$, where $A_0=L_xL_y=121\sigma^2$ is the interfacial area of the unperturbed state.

The WIM technique is an extension of the *NPT* ensemble in which the interfacial area is allowed to fluctuate at random. This is achieved by introducing a new MC move, which consists of an attempt to deform the box by changing the interfacial area of the system at constant volume. The attempted moves are accepted according to the usual canonical rules, and the surface tension may be extracted from the resulting surface area probability distribution. Further details can be found in Ref. 20. The WIM approach can also be implemented in the grand canonical ensemble (suitable for confined fluids) or in the canonical ensemble; the latter is a better option for the description of vapor-liquid or liquid-liquid interfaces. For the special case of discrete sampling of the surface area, the WIM technique becomes equivalent to the recent expanded ensemble methodology.[8,22]

For each chain length, we perform simulations of inhomogeneous systems at different temperatures where vapor-liquid equilibrium is expected. We typically consider either six or seven temperatures in the range from ~0.5 to ~0.9 T_c, where T_c is the critical temperature of the system. Each series is started at an intermediate temperature. This system is well equilibrated for 10^6 MC cycles, and averages are determined over a further period of 2×10^6 MC cycles. The systems at other temperatures of each series are equilibrated for 5×10^5 MC cycles and averages are determined over the same number of cycles (2×10^6). The production stage is divided into M blocks. The ensemble average of the surface tension is obtained from the arithmetic mean of the block averages, and the statistical precision of the sample average is estimated from the standard deviation of the ensemble average from $\bar{\sigma}/\sqrt{M}$, where $\bar{\sigma}$ is the variance of the block averages. We consider $M=20$, but in some cases averages are taken over more blocks.

All the quantities in our paper are expressed in conventional reduced units, with σ and ϵ being the length and en-

ergy units, respectively. Thus, the temperature is given in units of ϵ/k_B, the densities in units of σ^{-3}, the surface tension in units of ϵ/σ^2, and the interfacial thickness in units of σ.

III. RESULTS AND DISCUSSION

In this section we present the main results from the simulations of fully flexible LJ chains of varying chain length. We first focus on the interfacial properties such as density profiles, interfacial thickness, and surface tension, considering a cutoff distance of $r_c=4\sigma$ for the segment-segment interactions. In particular, we examine the temperature and chain length dependence of these properties. In the last section we examine the effect of the truncation of the interactions on the interfacial properties.

A. Interfacial properties of Lennard-Jones chains with $r_c=4\sigma$

We follow the same procedure for all chain lengths and temperatures. The equilibrium density profiles $\rho(z)$ are computed from averages of the histogram of densities along the z direction over the production stage. For convenience, density profiles are presented in terms of the monomeric units. As a consequence of our initial setup, the system stabilizes two planar vapor-liquid interfaces parallel (on average) to the x-y plane. The bulk vapor and liquid densities are obtained by averaging $\rho(z)$ over appropriate regions sufficiently removed from the interfacial region. This procedure is meaningful as far as the central liquid slab is thick enough. This turns out to be the case in our simulations, including those performed at the higher temperatures. The bulk vapor density is obtained after averaging the density profiles on both sides of the liquid film. The statistical uncertainty of these values is estimated from the standard deviation of the mean values. Additional interfacial properties can be determined by describing each of the two equilibrium density profiles to hyperbolic tangent functions of the form

$$\rho(z)=\frac{1}{2}(\rho_L+\rho_V)-\frac{1}{2}(\rho_L-\rho_V)\tanh\left(\frac{z-z_0}{d}\right), \tag{3}$$

where ρ_L, ρ_V, and z_0 are, in general, adjustable parameters corresponding to the liquid and vapor densities at coexistence, and the position of the Gibbs dividing surface. d is a measure of the thickness of the interface and it is related to the "10–90 interfacial thickness" (t) by $t=2.1972d$. Here we fix ρ_L and ρ_V to previously computed values and treat z_0 and d as adjustable parameters. As for the calculation of the bulk vapor density, our reported values of d correspond to the average of the values for the two interfaces appearing in the system. Values determined in this way are always found to be the same within statistical uncertainties; this suggests that the inhomogeneous systems are properly equilibrated at all temperatures.

We show in Fig. 1 the segment density profiles $\rho(z)$ for LJ chains formed from four monomers ($m=4$) at several temperatures in the vapor-liquid coexistence region. For the sake of clarity, we only present one half of the corresponding profiles corresponding to one of the interfaces (the full profiles are displayed as an inset in the figure). Also for convenience, all density profiles have been shifted along z so as to place z_0 at the origin. As can be seen in the inset of the figure, all profiles are essentially symmetric around the midpoint of the corresponding liquid slabs ($z\approx L_z/2\approx 36\sigma$), even for the longer chains considered here. As discussed earlier, this provides additional evidence that the inhomogeneous systems are properly equilibrated. Our simulation results for the bulk densities and interfacial thickness for LJ chains formed from four monomers are collected in Table I.

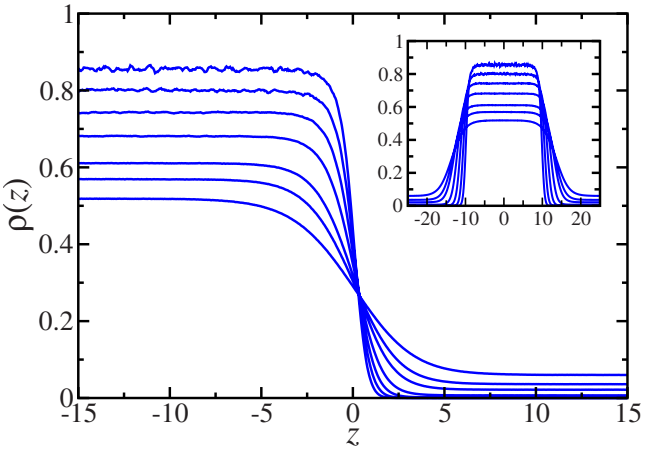

FIG. 1. (Color online) Simulated equilibrium density profiles across the vapor-liquid interface of fully flexible LJ chains formed from four monomers ($m=4$) with a segment-segment LJ cutoff distance of $r_c=4\sigma$ at several temperatures. From top to bottom (in the liquid region): $T=1.0$, 1.2, 1.4, 1.6, 1.8, 1.9, and 2.0. In the inset, the density profiles are shown with the liquid slab in the central part of the simulation box and the two vapor phases at each side of the liquid.

A similar analysis is used for the other chain lengths considered in this work. Bulk coexistence densities and interfacial thicknesses for chains formed from 8, 12, and 16 monomer segments are gathered in Tables II, III, and IV, respectively. The vapor densities and the interfacial thicknesses associated with both interfaces are nearly identical in all of the systems and at all temperatures, as found for the shortest chains with $m=4$. From the simulation data pre-

TABLE I. Liquid density ρ_L, vapor density ρ_V, surface tension γ, and 10–90 interfacial thickness t at different temperatures for systems of fully flexible LJ chains formed from four monomers with a segment-segment LJ cutoff of $r_c=4\sigma$. The surface tension is calculated using the TA method. All quantities are expressed in conventional reduced units as explained in Sec. II. The errors are estimated from the standard deviation of the mean. In the case of the surface tension, this is obtained from 20 subaverages, each consisting of 10^5 cycles. In the case of ρ_L and ρ_V, we use the values of the equilibrium density profile corresponding to the liquid and vapor regions, respectively. For the interfacial thickness, we use the two values obtained using Eq. (3) for the two interfaces in the simulation box.

T^*	ρ_L	ρ_V	γ	t
1.0	0.855(4)	0.000 009(3)	1.11(3)	1.657(2)
1.2	0.800(2)	0.000 20(1)	0.88(3)	2.059(4)
1.4	0.7428(9)	0.001 58(3)	0.67(2)	2.56(1)
1.6	0.6812(6)	0.006 93(4)	0.468(9)	3.278(2)
1.8	0.6108(3)	0.021 64(8)	0.281(6)	4.4419(4)
1.9	0.5692(3)	0.036 1(1)	0.194(8)	5.423(7)
2.0	0.5183(2)	0.060 0(1)	0.112(6)	7.090(4)

TABLE II. Liquid density ρ_L, vapor density ρ_V, surface tension γ, and 10–90 interfacial thickness t at different temperatures for systems of fully flexible LJ chains formed from eight monomers with a segment-segment LJ cutoff of $r_c=4\sigma$. The surface tension is calculated using the WIM technique. All quantities are expressed in the reduced units defined in Sec. II. The errors are estimated as explained in Table I.

T	ρ_L	ρ_V	γ	t
1.6	0.729(2)	0.000 17(1)	0.67(2)	2.599(9)
1.8	0.6789(8)	0.001 19(3)	0.47(2)	3.1735(1)
2.0	0.6225(5)	0.004 96(4)	0.33(2)	3.981(2)
2.2	0.5584(4)	0.015 62(7)	0.22(1)	5.245(2)
2.4	0.4745(3)	0.044 7(5)	0.083(9)	8.094(9)
2.5	0.3893(4)	0.086(4)	0.065(6)	12.876(4)

TABLE IV. Liquid density ρ_L, vapor density ρ_V, surface tension γ, and 10–90 interfacial thickness t at different temperatures for systems of fully flexible LJ chains formed from 16 monomers with a segment-segment LJ cutoff of $r_c=4\sigma$. The surface tension is calculated using the TA method. All quantities are expressed in the reduced units defined in Sec. II. The errors are estimated as explained in Table I.

T	ρ_L	ρ_V	γ	t
2.0	0.659(2)	0.000 12(1)	0.47(3)	3.197(2)
2.2	0.610(1)	0.000 79(3)	0.33(2)	3.817(2)
2.4	0.5570(6)	0.003 56(5)	0.22(1)	4.724(4)
2.6	0.4937(3)	0.012 24(8)	0.13(1)	6.29(1)
2.7	0.4542(3)	0.022 3(1)	0.10(1)	7.774(4)
2.8	0.3972(3)	0.043 5(2)	0.06(1)	10.99(9)

sented in Tables I–IV, one can compare the vapor-liquid phase envelope for LJ chains of different chain lengths. It is also useful to estimate the location of the critical point resulting from our direct MC simulations. The critical temperature T_c and density ρ_c are obtained using the simulation results of the vapor and liquid coexistence densities (Tables I–IV) and the scaling relation for the width of the coexistence curve

$$\rho_L - \rho_V = A(T - T_c)^{\beta} \tag{4}$$

and the law of rectilinear diameters

$$\frac{\rho_L + \rho_V}{2} = B + CT. \tag{5}$$

A, B, and C are constants, and β is the corresponding critical exponent. A universal value of $\beta=0.325$ is assumed here.[1] In Table V we report the values of the critical temperatures and densities as obtained from this procedure for all of the systems studied in this work.

The vapor-liquid phase envelopes of fully flexible LJ chains with $r_c=4\sigma$ are depicted in Fig. 2. Note that densities are again presented in terms of the monomeric segments. The coexistence envelopes exhibit a definite trend with chain length when represented in terms of the monomeric density. As can be seen in Fig. 2, the phase envelope becomes wider as the chain length is increased, as one would expect. The increase is more significant when the number of monomers is increased from four to eight than when the chain length is further increased. A similar behavior is also observed for the critical properties. This is consistent with the well-known asymptotic behavior of the vapor-liquid phase envelope of LJ chains expected as $m \to \infty$.[46]

Another interesting property obtained from our analysis is the 10–90 interfacial thickness (cf. Tables I–IV). For a given chain length, t is seen to increase with temperature, which simply reflects the fact that the interfacial region gets correspondingly wider. This can be observed in Fig. 1. At low temperatures the density profiles exhibit a sharp interface, which corresponds to a low value of the interfacial thickness. As the temperature is increased toward the critical value, the interfacial region becomes wider, and hence, the value of the interfacial thickness increases and diverges to infinity as $T \to T_c$. The variation in interfacial thickness with temperature for different chain lengths is illustrated in Fig. 3(a). According to the figure, increasing the chain length results in a decrease in the thickness of the interface at fixed temperature, which is consistent with the fact that the systems of longer molecules have a larger cohesive energy. This behavior is consistent with that found for the shape of the vapor-liquid phase envelopes. It is interesting to note that the variation in t with chain length at constant temperature is more significant for a change from $m=4$ to $m=8$ than in the rest of the cases. This is again related with the aforementioned asymptotic limit.

In Fig. 3(b) we show the 10–90 interfacial thickness of LJ chains as a function of temperature reduced by the appropriate critical temperature (T/T_c). This representation is par-

TABLE III. Liquid density ρ_L, vapor density ρ_V, surface tension γ, and 10–90 interfacial thickness t at different temperatures for systems of fully flexible LJ chains formed from 12 monomers with a segment-segment LJ cutoff of $r_c=4\sigma$. The surface tension is calculated using the WIM technique. All quantities are expressed in the reduced units defined in Sec. II. The errors are estimated as explained in Table I.

T	ρ_L	ρ_V	γ	t
1.8	0.698(2)	0.000 096(7)	0.60(4)	2.872(4)
2.0	0.648(1)	0.000 71(1)	0.41(2)	3.444(2)
2.2	0.5944(4)	0.003 20(4)	0.32(3)	4.254(4)
2.4	0.5336(3)	0.010 99(6)	0.20(2)	5.550(2)
2.6	0.4554(2)	0.033 9(4)	0.09(2)	8.40(1)
2.7	0.3795(2)	0.069(4)	0.061(7)	12.57(2)

TABLE V. Critical temperature obtained from the analysis of the computed surface tension data using Eq. (6) and fixing the critical exponent to $\mu=1.258$ or to $\mu=11/9$; critical temperature and density obtained from the analysis of the coexistence densities using Eqs. (4) and (5), respectively. All the results correspond to systems consisting of fully flexible LJ chains formed from m monomers with a segment-segment LJ cutoff of $r_c=4\sigma$. All quantities are expressed in the reduced units defined in Sec. II.

m	T_c [a]	T_c [b]	T_c [c]	ρ_c [c]
4	2.20(3)	2.18(4)	2.173(7)	0.265(5)
8	2.65(5)	2.64(5)	2.59(1)	0.234(7)
12	2.88(7)	2.87(7)	2.81(1)	0.217(7)
16	3.0(1)	3.0(1)	2.96(2)	0.20(1)

[a] $\mu=1.258$.
[b] $\mu=11/9$.
[c] Using Eqs. (4) and (5).

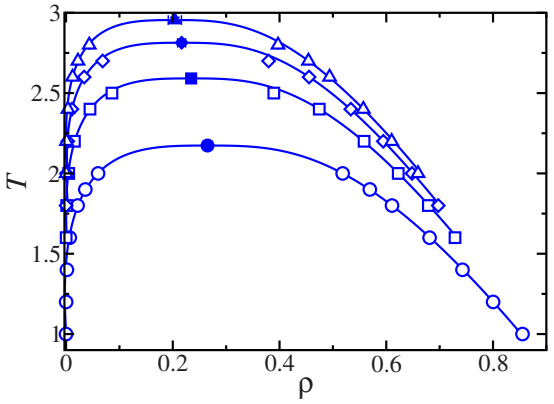

FIG. 2. (Color online) Vapor-liquid coexistence densities for fully flexible LJ chains with a segment-segment LJ cutoff distance of $r_c=4\sigma$. The open circles, squares, diamonds, and triangles correspond to the coexistence densities obtained from the analysis of the equilibrium density profiles obtained from MC *NVT* simulations for chain lengths of $m=4$, 8, 12, and 16, respectively. The filled symbols are the corresponding critical points estimated from Eqs. (4) and (5), and the curves represent the fits of the simulation data to Eq. (4).

ticularly useful when comparing interfacial properties of systems with different critical temperatures and, therefore, different ranges of temperatures over which vapor-liquid equilibria are observed. As can be seen, the values of the interfacial thickness of LJ chains with $m=8$, 12, and 16 are similar at all reduced temperatures. This would indicate that

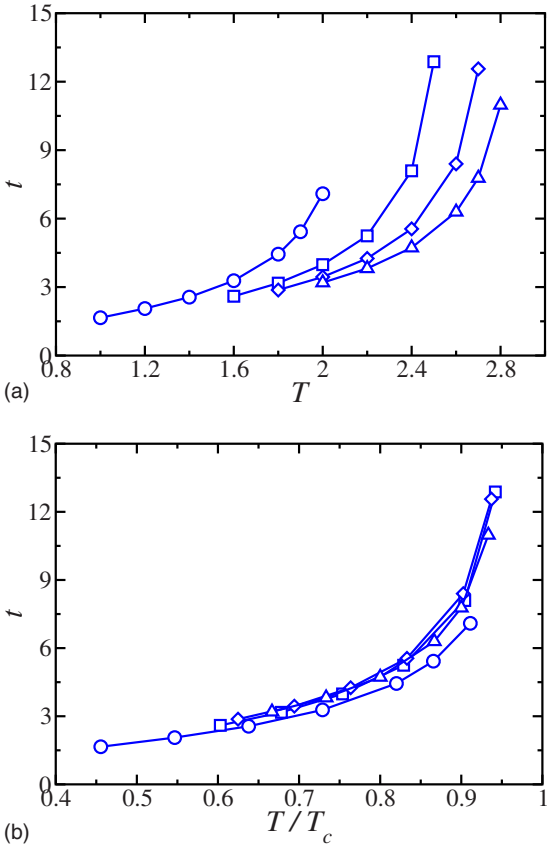

FIG. 3. (Color online) The 10–90 interfacial thickness t as a function of (a) the temperature and (b) the reduced temperature with respect to the critical point for fully flexible LJ chains with a segment-segment LJ cutoff distance of $r_c=4\sigma$. The meaning of the symbols is the same as in Fig. 2. The curves are included as a guide to the eyes.

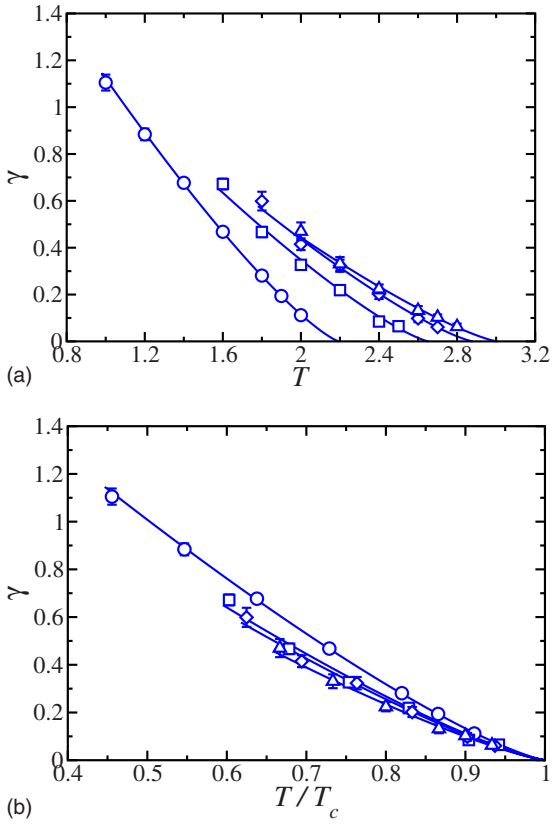

FIG. 4. (Color online) Surface tension as a function of (a) the temperature and (b) the reduced temperature with respect to the critical point for fully flexible LJ chains with a segment-segment LJ cutoff distance of $r_c=4\sigma$. The meaning of the symbols is the same as in Fig. 2. The curves represent the fits of the simulation data to the scaling relationship of the surface tension near the critical point given by Eq. (6) with $\mu=11/9$.

for fully flexible chains, the structure of the fluid in the interfacial region is largely dominated by monomer-monomer interactions, the chain length being an irrelevant parameter. It is interesting to note that our results are in qualitative agreement with those obtained by Bryk *et al.*[47] using a density functional theory approach.

Finally, the temperature dependence of the surface tension for the LJ chains is shown in Fig. 4(a). At any given temperature, the interfacial tension is larger for longer chains. Once again, this is consistent with the larger cohesive energy in systems consisting of long chains. As can be seen from Fig. 4(a), an essentially linear behavior is found for the range of temperatures considered here with a slight curvature close to the critical point for each system. The effect of chain length on the slope of the surface tension curves is remarkable. At a given temperature, this slope becomes less negative as m is increased, a trend which is also exhibited by the first members of the n-alkane series.[48] The same qualitative behavior has been previously found by Bryk *et al.*[47] One should bear in mind, however, that a fully flexible LJ chain model is not the most appropriate representation of real n-alkanes.

Though it would be of interest to compare our computed values of the surface tension to those recently reported by Duque *et al.*[38] for $m=4$, the comparison is not straightforward as the intermolecular interactions are slightly different.

TABLE VI. Liquid density ρ_L, vapor density ρ_V, surface tensions γ_{TA} and γ_{WIM}, and 10–90 interfacial thickness t at different temperatures for systems of fully flexible LJ chains formed from m monomers with a segment-segment LJ cutoff distance of r_c (in units of σ). The subscripts TA and WIM in γ indicate that the surface tension is calculated using the TA method and WIM technique, respectively. All quantities are expressed in the reduced units defined in Sec. II. The errors are estimated as explained in Table I.

m	T	r_c	ρ_L	ρ_V	γ_{TA}	γ_{WIM}	t
4	1.2	3	0.790(2)	0.000 320(1)	0.76(2)	0.75(2)	2.106(2)
4	1.2	4	0.800(2)	0.000 201(2)	0.88(2)	⋯	2.04(4)
4	1.2	5	0.803(2)	0.000 167(2)	0.90(1)	⋯	2.0813(1)
4	1.9	3	0.5355(2)	0.053 1(1)	0.132(5)	0.111(9)	6.489(1)
4	1.9	4	0.5692(3)	0.036 07(8)	0.194(7)	⋯	5.423(7)
4	1.9	5	0.5787(2)	0.031 750(1)	0.216(5)	⋯	5.254(2)
8	1.8	3	0.6628(7)	0.002 060(1)	0.42(1)	0.40(1)	3.300(2)
8	1.8	4	0.6789(8)	0.001 190(5)	⋯	0.47(2)	3.1735(1)
8	1.8	5	0.6836(8)	0.000 5(4)	⋯	0.49(2)	3.113(4)
8	2.2	3	0.5269(3)	0.026 24(8)	0.144(6)	0.125(9)	6.080(4)
8	2.2	4	0.5584(4)	0.015 62(1)	⋯	0.22(1)	5.245(2)
8	2.2	5	0.5681(3)	0.013 165(1)	⋯	0.27(1)	5.049(4)
12	2.0	3	0.6299(9)	0.001 430(1)	0.35(2)	0.33(1)	3.606(4)
12	2.0	4	0.648(1)	0.000 705(5)	⋯	0.41(2)	3.444(2)
12	2.0	5	0.654(1)	0.000 555(5)	⋯	0.51(3)	3.38(1)
12	2.4	3	0.4987(2)	0.020 52(2)	0.148(6)	0.131(9)	6.534(9)
12	2.4	4	0.5336(3)	0.010 99(3)	⋯	0.20(2)	5.550(2)
12	2.4	5	0.5440(3)	0.008 84(3)	⋯	0.21(2)	5.313(4)
16	2.2	3	0.5905(9)	0.001 77(1)	0.26(2)	0.27(2)	4.15(2)
16	2.2	4	0.610(1)	0.000 785(5)	0.33(2)	⋯	3.817(2)
16	2.2	5	0.617(1)	0.000 60(1)	0.40(2)	⋯	3.81(1)
16	2.7	3	0.4720(2)	0.016 52(2)	0.078(8)	0.066(6)	13.2(2)
16	2.7	4	0.4542(3)	0.022 3(1)	0.10(1)	⋯	7.776(4)
16	2.7	5	0.4720(2)	0.016 52(2)	0.11(1)	⋯	7.13(2)

While we make use of ST interactions, Duque *et al.*[38] consider truncated intermolecular forces, which are known to be equivalent to a spherically truncated *and shifted* (STS) version of the intermolecular interactions.[49] All other factors being equal, this difference should result in slightly higher values of the interfacial tension for the ST models when compared to the STS models. Our value of cutoff distance, $r_c=4\sigma$, is also smaller than the value of $r_c=6\sigma$ considered by Duque *et al.*;[38] larger values of the truncation distance are expected to yield larger values of the surface tension. These two differences therefore give rise to opposing trends. We find that the values of the interfacial tension obtained by Duque *et al.*[38] are higher than ours at higher and lower temperatures, whereas our values are slightly higher for intermediate temperatures.

The representation shown in Fig. 4(a) suggests a convergence of the surface tension with increasing chain length; the asymptotic regime has not, however, yet been attained for the moderate chain lengths considered in this work. This behavior is in agreement with experimental results for the homologous series of chain molecules such as polysiloxane.[50] We show in Fig. 4(b) the computed values of the surface tension in terms of the temperature reduced by the corresponding critical value (T/T_c). As can be seen in Fig. 4(b), the surface tension decreases as the chain becomes longer at any given reduced temperature. As mentioned earlier, the slope of the curves becomes less negative with increasing chain length. As found for the interfacial thickness, the surface tension exhibits a clear asymptotic behavior with increasing m.

The computed values of the surface tension allow us to obtain an independent estimate of the critical temperature for each chain length from the scaling relation

$$\gamma = \gamma_0(1 - T/T_c)^{\mu}, \tag{6}$$

where γ is the surface tension at temperature T, γ_0 is the "zero-temperature" surface tension, μ is the corresponding critical exponent, and T_c is the critical temperature. Here, we fix μ to the universal value of $\mu=1.258$ as obtained from renormalization-group theory.[1] We also use the empirical value $\mu=11/9$ suggested by Guggenheim.[51] Our estimates for the critical temperatures are collected in Table V. The overall agreement between these values and those obtained from an analysis of the coexistence densities is consistent.

B. Effect of the cutoff distance on the interfacial properties of Lennard-Jones chains

We have performed a preliminary study on the effect of truncating the interactions on the different thermodynamic and interfacial properties. We consider for this purpose simulations at selected temperatures for two additional values of the cutoff distance, $r_c=3$ and 5σ, using the same setup as the one used in the preceding sections. The corresponding results are summarized in Table VI. For the shorter cutoff distance, $r_c=3\sigma$, we have calculated the surface tension using the TA method and the WIM technique. As can be seen, both methodologies provide consistent values for the surface tension of all the systems.

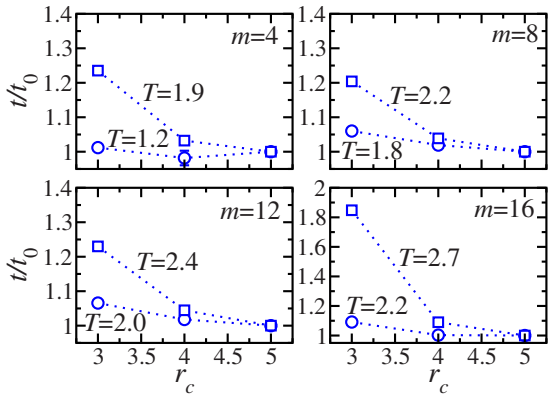

FIG. 5. (Color online) Reduced interfacial thickness t/t_0 as a function of the segment-segment LJ cutoff distance r_c for fully flexible LJ chains at two different temperatures. t_0 is the interfacial thickness corresponding to $r_c=5\sigma$. The lower values of t/t_0 (circles) correspond to the lower temperatures and the higher (squares) correspond to the higher temperatures presented in Table VI for each system. The lines are included as a guide to the eyes.

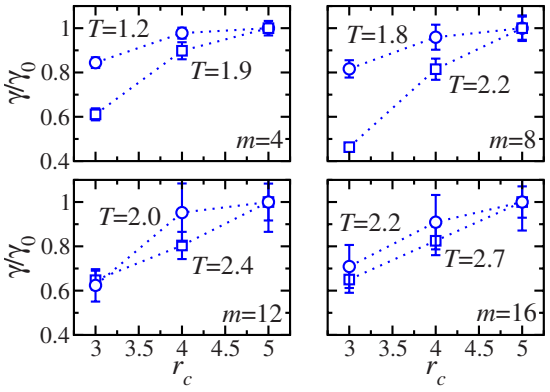

FIG. 6. (Color online) Reduced surface tension γ/γ_0 as a function of the segment-segment LJ cutoff distance r_c for fully flexible LJ chains at two different temperatures. γ_0 is the interfacial thickness corresponding to $r_c=5\sigma$. The higher values of γ/γ_0 (circles) correspond to the lower temperatures and the lower (squares) correspond to the higher temperatures presented in Table VI for each system. The lines are included as a guide to the eyes.

We start by considering the effect on the coexistence densities. As can be seen in Table VI at low and high temperatures the liquid density increases and the vapor density decreases as r_c is increased. This results in the well-known widening of the coexistence curve as r_c becomes larger. Our results indicate that the changes in the vapor density are larger than those corresponding to the liquid density, and the effect of the cutoff distance on the coexistence densities is more pronounced for the systems of longer chains. We have also considered the effect on the 10–90 interfacial thickness, t, which is more sensitive to changes in the cutoff than the coexistence densities. In Fig. 5 we show the interfacial thickness as a function of the cutoff distance for all the systems considered. As can be seen, the interfacial thickness decreases as r_c is increased, in agreement with our previous results. We observe that changes in t, when r_c is varied from 3 to 5σ, are larger at high temperatures and for longer chains. In particular, the interfacial thickness decreases in value between 1% and 8% at low temperatures and between 17% and 46% at high temperatures.

Finally, we analyze the effect of the cutoff distance on the surface tension γ. As can be seen in Fig. 6, the surface tension is very sensitive to the precise value of the cutoff distance. As one would expect, the surface tension becomes larger as the cutoff distance is increased. In general, the effect is more marked at higher than at lower temperatures. In addition, the changes in surface tension for a given change in the cutoff distance also exhibit a strong dependence with the chain length. In particular, the change in γ varies from 19% at low temperatures and short chains up to ~60% at high temperatures and long chains.

IV. CONCLUSION

We have simulated the interfacial properties of the vapor-liquid interface of fully flexible chains formed from tangentially bonded LJ monomers. Chains formed from 4, 8, 12, and 16 monomers are considered. The intermolecular and intramolecular segment-segment interactions are truncated at a cutoff distance of 4σ, σ being the diameter of the monomers. We use MC *NVT* simulation of the inhomogeneous system containing two vapor-liquid interfaces. The surface tension is evaluated using the TA approach and the WIM technique. We have examined the density profiles, interfacial thickness, and surface tension in terms of the temperature and the number of monomers forming the chains. In addition, we have also calculated the coexistence phase envelope, including the location of the critical point from an analysis of the density profiles and the surface tension.

The effect of the chain length on the density profiles, coexistence densities, critical temperature and density, interfacial thickness, and surface tension has been investigated. The vapor-liquid interface is seen to sharpen with increasing chain length corresponding to an increase in the width of the coexistence phase envelope and an accompanying increase in the surface tension.

The coexistence phase envelope, the interfacial thickness, and the surface tension are seen to exhibit an asymptotic limiting behavior as the chains get longer. In particular, when the interfacial thickness and surface tension are plotted as functions of the reduced temperature T/T_c, both properties exhibit a nearly universal behavior for chains formed from eight or more monomers. This indicates that the interface, hence its thickness and associated surface tension, is dominated by monomer-monomer interactions, irrespective of the number of monomers constituting the molecular chain.

Finally, we have also presented the results of an analysis of the effect of truncation of the LJ interactions on the interfacial properties. In particular, the results for a number of properties are compared for values of the cutoff distance of 3, 4, and 5σ at two different temperatures. All properties exhibit a dependence with the cutoff distance, but the relative effect is different depending on the specific property. Though the density profiles and coexistence densities are affected by the cutoff distance, the interfacial thickness and more particularly the surface tension show a stronger dependence on the particular choice of cutoff distance.

ACKNOWLEDGMENTS

F.J.B. and E.dM. acknowledge financial support from the Spanish Dirección General de Investigación (Project No. FIS2007-66079-CO2-02) and the Proyecto de Excelencia from Junta de Andalucía (Grant No. P07-FQM02884). Additional support from Universidad de Huelva and Junta de Andalucía is also acknowledged. L.G.M. would like to acknowledge financial support from Santander-UCM (Project No. PR34/07-15906), MEC (Grant No. FIS2007-66079-C02-01), and CAM (Grant No. S-0505/ESP/000299). G.J. acknowledges financial support from the Engineering and Physical Sciences Research Council (EPSRC) of the UK (Grant Nos. GR/N20317, GR/N03358, GR/N35991, GR/R09497, and EP/E016340), the Joint Research Equipment Initiative (JREI) (Grant No. GR/M94427), and the Royal Society-Wolfson Foundation for a refurbishment grant.

[1] J. S. Rowlinson and B. Widom, *Molecular Theory of Capillarity* (Dover, New York, 2002).
[2] D. Henderson, *Fundamentals of Inhomogeneous Fluids* (Dekker, New York, 1992).
[3] H. T. Davis, *Statistical Mechanics of Phases, Interfaces, and Thin Films* (VCH, Weinheim, 1996).
[4] M. P. Allen and D. J. Tildesley, *Computer Simulation of Liquids* (Claredon Press, Oxford, 1987).
[5] D. Frenkel and B. Smit, *Understanding Molecular Simulations*, 2nd ed. (Academic, San Diego, 2002).
[6] M. Müller and L. G. MacDowell, Macromolecules **33**, 3902 (2000).
[7] G. J. Gloor, G. Jackson, F. J. Blas, and E. de Miguel, J. Chem. Phys. **123**, 134703 (2005).
[8] J. R. Errington and D. A. Kofke, J. Chem. Phys. **127**, 174709 (2007).
[9] J. G. Kirkwood and F. P. Buff, J. Chem. Phys. **17**, 338 (1949).
[10] J. H. Irving and J. G. Kirkwood, J. Chem. Phys. **18**, 817 (1950).
[11] R. Eppenga and D. Frenkel, Mol. Phys. **52**, 1303 (1984).
[12] V. I. Harismiadis, J. Vorholz, and A. Z. Panagiotopoulos, J. Chem. Phys. **105**, 8469 (1996).
[13] H. L. Vörtler and W. R. Smith, J. Chem. Phys. **112**, 5168 (2000).
[14] E. de Miguel and G. Jackson, J. Chem. Phys. **125**, 164109 (2006).
[15] K. Binder, Phys. Rev. A **25**, 1699 (1982).
[16] P. Virnau and M. Müller, J. Chem. Phys. **120**, 10925 (2004).
[17] C. H. Bennett, J. Comput. Phys. **22**, 245 (1976).
[18] J. Miyazaki, J. A. Barker, and G. M. Pound, J. Chem. Phys. **64**, 3364 (1976).
[19] E. Salomons and M. Mareschal, J. Phys.: Condens. Matter **3**, 3645 (1991).
[20] L. G. MacDowell and P. Bryk, Phys. Rev. E **75**, 061609 (2007).
[21] A. P. Lyubartsev, A. A. Martsinovski, S. V. Shevkunov, and P. N. Vorontsov-Velyaminov, J. Chem. Phys. **96**, 1776 (1992).
[22] E. de Miguel, J. Phys. Chem. B **112**, 4674 (2008).
[23] C. Vega and E. de Miguel, J. Chem. Phys. **126**, 154707 (2007).
[24] E. de Miguel, N. G. Almarza, and G. Jackson, J. Chem. Phys. **127**, 034707 (2007).
[25] C. Ibergay, A. Ghoufi, F. Goujon, P. Ungerer, A. Boutin, B. Rousseau, and P. Malfreyt, Phys. Rev. E **75**, 051602 (2007).
[26] A. Ghoufi, F. Goujon, V. Lachet, and P. Malfreyt, Phys. Rev. E **77**, 031601 (2008).
[27] A. I. Milchev and A. A. Milchev, Europhys. Lett. **56**, 695 (2001).
[28] F. Varnik, J. Baschnagel, and K. Binder, J. Chem. Phys. **113**, 4444 (2000).
[29] P. Virnau, M. Müller, L. G. MacDowell, and K. Binder, J. Chem. Phys. **121**, 2169 (2004).
[30] B. M. Mognetti, L. Yelash, P. Virnau, W. Paul, K. Binder, M. Müller, and L. G. MacDowell, J. Chem. Phys. **128**, 104501 (2008).
[31] Y.-J. Sheng, A. Z. Panagiotopoulos, S. K. Kumar, and I. Szleifer, Macromolecules **27**, 400 (1994).
[32] Y.-J. Sheng, A. Z. Panagiotopoulos, and S. K. Kumar, Macromolecules **29**, 4444 (1996).
[33] F. A. Escobedo and J. J. de Pablo, Mol. Phys. **87**, 347 (1996).
[34] F. J. Blas and L. F. Vega, Mol. Phys. **92**, 135 (1997).
[35] C. Vega, F. J. Blas, and A. Galindo, J. Chem. Phys. **116**, 7645 (2002).
[36] C. Vega, C. McBride, E. de Miguel, F. J. Blas, and A. Galindo, J. Chem. Phys. **118**, 10696 (2003).
[37] A. Galindo, C. Vega, E. Sanz, L. G. MacDowell, E. de Miguel, and F. J. Blas, J. Chem. Phys. **120**, 3957 (2004).
[38] D. Duque, J. C. Pàmies, and L. F. Vega, J. Chem. Phys. **121**, 11395 (2004).
[39] C. Vega, E. P. A. Paras, and P. A. Monson, J. Chem. Phys. **96**, 9060 (1992).
[40] D. Frenkel, G. C. A. M. Mooij, and B. Smit, J. Phys.: Condens. Matter **3**, 3053 (1991).
[41] J. I. Siepmann and D. Frenkel, Mol. Phys. **75**, 59 (1992).
[42] J. J. de Pablo, M. Laso, and U. W. Suter, J. Chem. Phys. **96**, 2395 (1992).
[43] B. Smit, Mol. Phys. **85**, 153 (1995).
[44] L. G. MacDowell, "Termodinámica Estadística de Moléculas Flexibles: Teoría y Simulación," Ph.D. thesis, Universidad Complutense de Madrid, 2000.
[45] L. G. MacDowell, C. Vega, and E. Sanz, J. Chem. Phys. **115**, 6220 (2001).
[46] C. Vega and L. G. MacDowell, Mol. Phys. **98**, 1295 (2000).
[47] P. Bryk, K. Bucior, S. Sokolowski, and G. Zukocinski, J. Phys.: Condens. Matter **16**, 8861 (2004).
[48] G. J. Gloor, G. Jackson, F. J. Blas, E. M. del Río, and E. de Miguel, J. Phys. Chem. C **111**, 15513 (2007).
[49] A. Trokhymchuk and J. Alejandre, J. Chem. Phys. **111**, 8510 (1999).
[50] P. G. de Gennes, F. Brochard-Wyart, and D. Quéré, *Capillarity and Wetting Phenomena* (Springer, New York, 2004).
[51] E. A. Guggenheim, J. Chem. Phys. **13**, 253 (1945).